Turkish Journal of Electrical Engineering & Computer Sciences

http://journals.tubitak.gov.tr/elektrik/

Research Article

Turk J Elec Eng & Comp Sci
(2018) 26: 803 – 816

doi:10.3906/elk-1705-165

Upper envelope detection of ECG signals for baseline wander correction: a pilot study

Mohammed Assam OUALI[1,2,*], **Mouna GHANAI**[1], **Kheireddine CHAFAA**[1]
[1]Laboratory of Advanced Automatics and Systems Analysis (LAAAS), Department of Electronics, Faculty of Technology, Mostefa Ben Boulaid University, Batna 2, Algeria
[2]GREYC Laboratory, University of Caen, Caen, France

Received: 14.05.2017 • **Accepted/Published Online:** 18.12.2017 • **Final Version:** 30.03.2018

Abstract: Baseline wander (BW) is a common low frequency artifact in electrocardiogram (ECG) signals. The prime cause from which BW arises is the patient's breathing and movement. To facilitate reliable visual interpretation of the ECG and to discern particular patterns in the ECG signal, BW needs to be removed. In this paper, a novel BW removal method is presented. The hypothesis is based on the observation that ECG signal variation covaries with its BW. As such, the P, Q, R, S, and T peaks will follow the baseline drift. On this basis, the following proposition is true: a reliable approximation of the baseline drift can be obtained from the shape derived from the interpolation of one form of the ECG signal peak (peak envelope). The simulation was performed by adding artificial BW to ECG signal recordings. The signal-to-noise ratio, mean squared error, and improvement factor criteria were used to numerically evaluate the performance of the proposed approach. The technique was compared to that of the Hilbert vibration decomposition method, an empirical-mode decomposition technique and mathematical morphology. The results of the simulation indicate that the proposed technique is most effective in situations where there is a considerable distortion in the baseline wandering.

Key words: Electrocardiogram, baseline wandering, cubic spline interpolation, R-peak detection.

1. Introduction

The purpose of an electrocardiogram (ECG) is to measure the electrical potential changes in the heart over a specific time period. Particular cells in the heart produce electrical impulses that spread through the heart, causing it to contract and thereby controlling the heartbeat rate and causing these changes in the electrical potentials [1–4]. In an ECG, these electrical changes are measured through electrodes positioned on the chest. The electrical impulses are recorded in millivolts, while the idealized heartbeat comprises a number of complexes, three of which are frequently recorded and utilized in medical ECG terminology. These are the P complex, which measures the depolarization of the atrium; the QRS complex, which measures the depolarization of the ventricles; and the T complex, which measures the repolarization of the ventricles. ECGs are extensively used for diagnosis of heart diseases. It is also an essential tool that allows monitoring patients at home, thereby advancing telemedical applications. Recent contributions to this topic were reported in [5–7]. However, the ECG signal frequently becomes contaminated by both internal and external noises. While there are numerous sources of these noises, the ones of primary interest are instrument and EMG noises, electrode contact noise,

*Correspondence: mohammed-assam.ouali@unicaen.fr

motion artifacts, and power line interference [8]. As such, it is necessary to carry out advanced digital processing of the ECG waveforms in order to utilize the electrocardiogram of an individual for identification and diagnosis purposes. Obviously, any noise that appears on the trace of the ECG can complicate diagnosis and identification analysis. Therefore, it is necessary to understand and cancel out the effects of noise from an ECG trace in order to extract the required identifying features of the trace itself.

The baseline is the heart's isoelectric line, which corresponds to an unchanging trace, meaning that the electrical potential is constant. Frequently, there is poor placement or contact between the electrodes and the patient's skin; this results in relative motion of the electrode to the skin as the patient's chest expands and contracts during breathing. This leads to baseline drift [9–12]. The frequency range of the baseline wander (BW) is usually less than 1.0 Hz; however, for exercise ECG this range can be wider [9,13,14]. For reliable ECG interpretation, it is crucial for the BW to be corrected without disturbing the underlying cardiological signals.

This work deals with the problems of BW reduction. Generally, methods used to reduce this kind of disturbance can be divided into two groups: methods based on BW estimation and methods based on high-pass filtering. The first approach will be adopted in this paper. The second approach (high-pass filters) would unavoidably introduce distortions in various parts of the ECG signal, especially in the ST segment due to the spectra of the ST segment that overlap the spectra of the BW [15,16]. In this paper the estimation of the BW can be obtained from the shape derived from the interpolation of one form of the ECG signal peak (peak envelope). The contributions of this work lie in the aspect of using the cubic spline interpolation with ECG peaks to remove the BW noise without introducing any distortions into the ECG signal.

Several methods of removing this noise from ECG signals were proposed in the literature. These methods include Hilbert vibration decomposition (HVD), in which the highest energy component of the HVD that was the first component corresponds to the BW signal [17]. In [18] BW was removed by using a novel technique based on quadratic variation reduction. In [19] fractal modeling was used to create a projection operator that allows BW removal. The authors of [20] used a system of jointly modeled PI and BW to remove the noise of biopotential signals. With this method, the BW was modeled by a set of harmonically related sinusoids modulated by low-order time polynomials [20]. In another study, the empirical mode decomposition technique was used with a low-pass filter that had been devised from the averages of opening and closing operators [8]. Many other approaches have been reported in the literature to address the problem of ECG enhancement [18,21–29].

This study focuses on modeling and removing the BW noise from the ECG signal by using the shape derived from R-peaks via cubic spline interpolation. The performance of the proposed algorithm is demonstrated through various experiments performed over several records from the MIT–BIH arrhythmia database [30] and synthetic ECG signals [31]. Quantitative and qualitative experiments are carried out for synthetic and real BW noises. Comparative study of the proposed approach with recently published benchmark methods of BW drift correction is also performed. All these experiments show that the proposed method is a good tool for BW removal.

This paper is divided into five sections. After this introduction section, Section 2 outlines the notion of the extrema, the cubic spline interpolation method, and the ECG signal used in the experimentation. The proposed technique is introduced in Section 3. Section 4 presents a number of experimental examples to verify the effectiveness of the proposed method and a comparative study. Finally, conclusions are given in Section 5.

2. Preliminaries

2.1. Extrema

The extrema of the function f are the minimum and maximum values on a graph. The derivative, or gradient, of a function $x = f(t)$ represents the rate of change, denoted by dx/dt or $\nabla x(t)$. Mathematically, this represents the slope of the tangent to the curve $x = f(t)$ at a given point t. Much can be deduced about the curve by determining the derivative value at each time. Note that when $\frac{dx}{dt} = 0$, the slope of the tangent to the curve is horizontal; therefore, the curve is said to have a stationary point.

Three types of stationary points may be encountered: local maxima, local minima, and horizontal points of inflection. As evident from their description, local maxima and minima, or relative maxima and minima, are localized extrema (Table 1; Figure 1).

Table 1. Local maxima and minima criteria.

Local minima	Local maxima
The stationary point at $t = t_2$ (see Figure 1) satisfies: $\frac{dx}{dt} < 0$ for $t < t_2$ $\frac{dx}{dt} = 0$ for $t = t_2$ and $\frac{dx}{dt} > 0$ for $t > t_2$ We have then a local minimum at $t = t_2$	The stationary point at $t = t_5$ (see Figure 1) satisfies: $\frac{dx}{dt} > 0$ for $t < t_5$ $\frac{dx}{dt} = 0$ for $t = t_5$ and $\frac{dx}{dt} < 0$ for $t > t_5$ We have then a local maximum at $t = t_5$

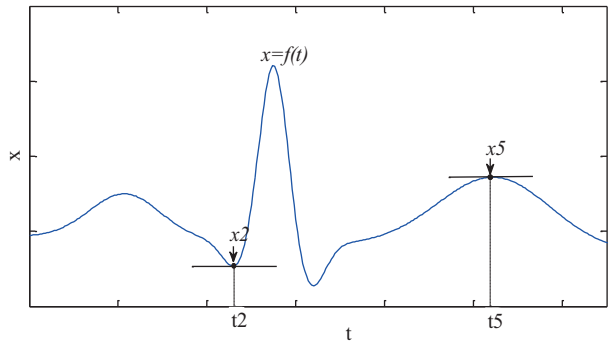

Figure 1. Extrema on ECG graph $x = f(t)$.

2.2. Cubic spline interpolation

Cubic spline interpolation smooths curves without adding irregularities to the signal and therefore it was selected as an appropriate technique to apply to the data.

Assuming that there are $n + 1$ points on an interval $[a,\ b]$ [32]:

$$\Delta : a = x_0 < x_1 < \cdots < x_n = b. \tag{1}$$

Let $S_i(x)$ be a cubic polynomial on each of the intervals $[x_i,\ x_{i+1}]$, so that we have n different polynomials of this type in total. According to the definition of the cubic spline interpolation, $S_i(x)$ can be represented by the following form:

$$S_i(x) = a_{0i} + a_{1i}x + a_{2i}x^2 + a_{3i}x^3 + \sum_{j=1}^{n-1} b_j (x - x_j)^3/6 \qquad a \le x \le b, \tag{2}$$

where $b_j = S^{'''}(x_j)$, $j = 1, 2, \cdots, n-1$, and $a_{0i}\, a_{1i}$, a_{2i}, a_{3i} are undetermined coefficients.

Since $S_i(x)$ is a second-order smooth polynomial, a three-moment interpolation will be used to calculate the equations. Then $S_i(x)$ can be rewritten in the following form:

$$S_i(x) = \frac{(x_{j+1} - x)^3}{6h_{j+1}} M_j + \frac{(x - x_j)^3}{6h_{j+1}} M_{j+1} + \frac{x - x_j}{h_{j+1}} \left(f_{j+1} - f_j - \frac{h_{j+1}^2}{6} (M_{j+1} - M_j) \right) + f_j - \frac{h_{j+1}^2}{6} M_j \tag{3}$$

with $h_{j+1} = x_{j+1} - x_j$, $j = 0, 1, \cdots, n-1$ and M_j is an undetermined parameter.

2.3. ECG signals

In this investigation two types of ECG signals will be used to test the effectiveness of the proposed method: 1) synthetic electrocardiograms generated by an ECG dynamical model [31], and 2) real electrocardiograms taken from the MIT–BIH database [30]. In the case of the synthetic ECG signals, a BW-free ECG record is corrupted by a priori known BW; therefore the quality of BW removal can be measured in terms of the corresponding estimation error, as will be shown below. For real signals, the quality of the BW removal is evaluated by a visual qualitative comparison of the corresponding detrended signals, since the wandering affecting the true signal is not known.

2.3.1. ECG dynamical model

McSharry et al. [31] proposed a synthetic ECG dynamical generator constituted of three-dimensional state equations (see Eq. (4)), which can generate a trajectory in the Cartesian coordinates:

$$\begin{aligned} \dot{x} &= \alpha x - \omega y, \\ \dot{y} &= \alpha y + \omega x, \\ \dot{z} &= -\sum_i a_i \Delta\theta_i \exp\left(-\frac{\Delta\theta_i^2}{2b_i^2}\right) - (z - z_0), \end{aligned} \tag{4}$$

where $\alpha = 1 - \sqrt{x^2 + y^2}$, $\Delta\theta_i = (\theta - \theta_i) mod(2\pi)$, $\theta = atan2(xy)$ ($atan2$ is the four quadrant arctangent of the real parts of the elements of x and y), with $-\pi \le atan2(x, y) \le \pi$, and ω is the angular velocity of the trajectory as it moves around the limit cycle while a_i, b_i, and θ_i correspond to amplitude, width, and center parameters of the Gaussians, respectively.

This model has many adjustable parameters, which makes it adaptable to many normal and abnormal ECG signals.

The drift of the baseline with respiration can be represented by a sinusoidal component at the frequency of respiration added to the ECG signal.

The baseline drift of the synthetic ECG signal (modeled by Eq. (4)) has been added by using the extra term z_0, which is coupled with the respiratory frequency f_2 as follows:

$$z_0 = A \times \sin(2\pi f_2 t), \tag{5}$$

where f_2 is the respiratory frequency.

2.3.2. ECG signals database

ECG data are taken from the MIT–BIH database [30]. The MIT–BIH Arrhythmia Database contains 48 excerpts of 30 min each of two-channel ambulatory ECG recordings, obtained from 47 subjects studied by the BIH Arrhythmia Laboratory between 1975 and 1979. Twenty-three recordings were chosen at random from a set of 4000 ambulatory ECG recordings of 24 h each collected from a mixed population of inpatients (about 60%) and outpatients (about 40%) at Boston's Beth Israel Hospital; the remaining 25 recordings were selected from the same set to include the less common but clinically significant arrhythmias that would not be well represented in a small random sample.

The recordings were digitized at 360 samples per second per channel with 11-bit resolution over a range of 10 mV. Two or more cardiologists annotated each record independently; disagreements were resolved to obtain the computer-readable reference annotations for each beat (approximately 110,000 annotations in total) included with the database.

3. Materials and methods

The flowchart in Figure 2 depicts the stages of the experimental method of removing the BW from ECG signals.

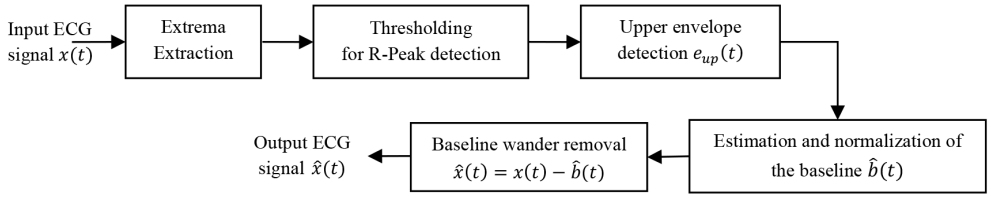

Figure 2. Complete BW removal pipeline.

The process commences by determining the extrema of the input ECG signal. The local maxima and minima were identified using the method described in Section 2.1. As the variation in the ECG signal tracks the BW, the P, Q, R, S, and T peaks will consistently follow the same shape as the baseline drift. This leads us to the following proposition:

Proposition

Among all ECG waves (P, Q, R, S, and T), let us consider the R-waves due to their high amplitude and fast variation as well as being quite resistant to noise.

The shape derived from the interpolation of the peaks of the R-waves (peaks envelope) is a suitable estimate for the BW.

Therefore, an R-peak detection algorithm will be needed. Such an algorithm comprises two stages:

1. Identification of the maxima and minima of the ECG data by using the stationary point approach outlined in Section 2.1.
2. Use of a trial and error approach to find a threshold in the ECG amplitude to isolate R-peaks from other peaks. As a perspective, we propose here the use of an automatic method for R-peaks detection like the Pan and Tompkins method [33].

Having determined the R-peaks, a cubic spline curve (see Section 2.2) is used to interpolate the R-peaks in order to obtain the upper envelope $e_{up}(t)$, which is assumed to have the form of the BW. The upper envelope

$e_{up}(t)$ represents a shifted form of the BW signal $\hat{b}(t)$ to be estimated. By subtracting the difference between the means of the upper envelope and ECG signal from the upper envelope, an estimate of the BW can be determined as indicated by:

$$\hat{b}\left(t\right) = e_{up}\left(t\right) - \left(mean\left(e_{up}\left(t\right)\right) - mean\left(x\left(t\right)\right)\right), \tag{6}$$

where $\hat{b}(t)$ is the estimate of the BW signal, $e_{up}(t)$ is the detected upper envelope, and $x(t)$ is the corrupted ECG signal containing the BW.

The BW in an ECG signal is modeled as a low-frequency additive noise [34,35]; therefore, an estimate of the clean ECG signal $\hat{x}(t)$ can be derived from the straightforward subtraction of the BW signal $\hat{b}(t)$ from the corrupted ECG signal $x(t)$ as follows:

$$\hat{x}\left(t\right) = x\left(t\right) - \hat{b}\left(t\right) \tag{7}$$

4. Results and discussion

In this section, simulation and experimental tests on both synthetic and real ECG signals are carried out to evaluate the performance of the proposed method.

For evaluation purposes, input signal to noise ratio (SNR), output SNR, the mean squared error (MSE) criterion, and the improvement factor (Imp) will be used. These evaluators are defined as follows:

- Input SNR:

$$SNR_{input} = 10 \times log\left(\frac{\sum\limits_{i}\left|x_c\left(i\right)\right|^2}{\sum_i\left|b\left(i\right)\right|^2}\right), \tag{8}$$

- Output SNR:

$$SNR_{output} = 10 \times \log\left(\frac{\sum\limits_{i}\left|x_c\left(i\right)\right|^2}{\sum_i\left|x_c\left(i\right) - \hat{x}(i)\right|^2}\right), \tag{9}$$

- Improvement factor (Imp):

$$imp\left[dB\right] = SNR_{output} - SNR_{input}, \tag{10}$$

- MSE:

$$MSE = \sum_{i}\left(x_c\left(i\right) - \hat{x}(i)\right)^2, \tag{11}$$

where x_c is the clean ECG signal, $\hat{x}$ is the estimated ECG signal, and b is the baseline wandering noise.

Table 2. Parameters of the synthetic ECG model (Eq. (4)).

Index (i)	P	Q	R	S	T
$Time\,(s)$	-0.2	-0.05	0	0.05	0.3
θ_i (rad)	$-\pi/3$	$-\pi/12$	0	$\pi/12$	$\pi/2$
A_i	20	-50	300	-75	75
b_i	0.25	0.1	0.1	0.1	0.4

4.1. Baseline wander removal from a synthetic ECG signal

The considered ECG signal is generated according to the model given in Eq. (4) with a period of 1 s. The parameters of this synthetic ECG signal are given in Table 2. Let us now introduce BW with amplitude of 0.15 mV and respiratory frequency f_2 equal to 0.25 Hz (see Eq. (5)).

The starting point of our approach is the determination of all extrema of the ECG signal. In this investigation, local minima and local maxima of the ECG signal are identified efficiently as shown in Figure 3 using the stationary point approach discussed in Section 2.1.

The second step of the method is to separate the R-peaks from the other peaks by applying a thresholding on the considered ECG signal amplitude as shown in Figure 4.

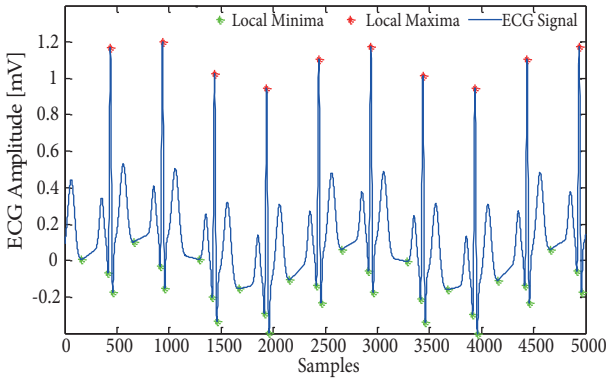

Figure 3. Maxima and minima identification of a synthetic ECG with the parameters of Table 2.

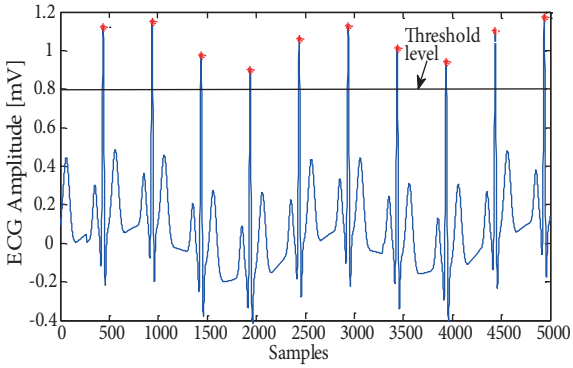

Figure 4. Synthetic ECG with detected R-peaks and thresholding.

Once the R-peaks are obtained, they will be interpolated by a cubic spline curve, which will give us the upper envelope $e_{up}(t)$ having the shape of the BW (see Figure 5).

As shown in Section 3, the detected upper envelope $e_{up}(t)$ represents a shifted version of the BW signal $\hat{b}(t)$; however, the BW estimate is obtained using Eq. (6). Therefore, and as shown in the Figure 6, an excellent BW estimate is obtained.

Finally, the BW is removed from the corrupted ECG by using Eq. (7), and the result is shown in Figure 7, where it can be seen that the proposed method has an excellent ability to remove the BW distortion.

To evaluate quantitatively the performance of the proposed method, we have used the SNR, MSE, and Imp criteria as shown in Table 3, in which significant improvements are noted.

Note that the BW and ECG signal have overlapping bands in the low frequency region of their spectra [36]. Unfortunately, distortion in this band negatively affects the shape of the ST segment, which is the portion connecting the QRS complex with the T-wave. The ST segment has strong clinical relevance, since deviations

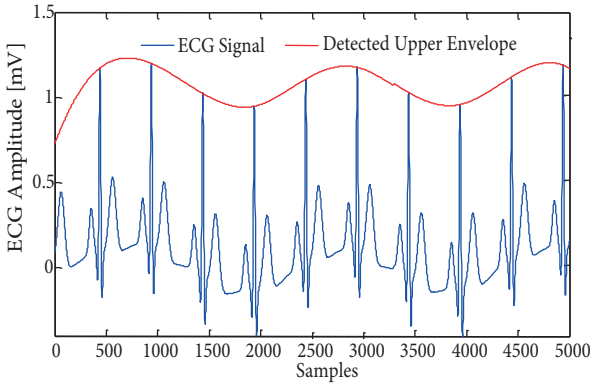

Figure 5. Synthetic ECG signal with its detected upper envelope.

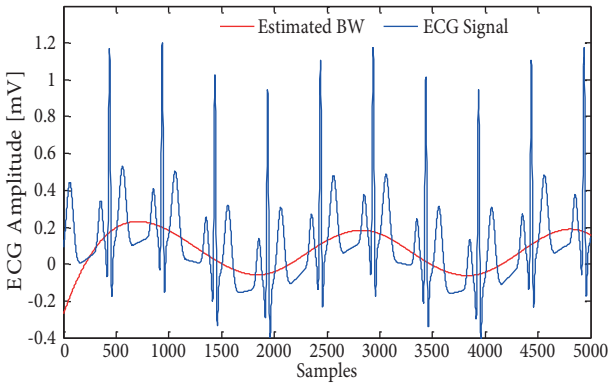

Figure 6. Synthetic ECG signal with its estimated BW.

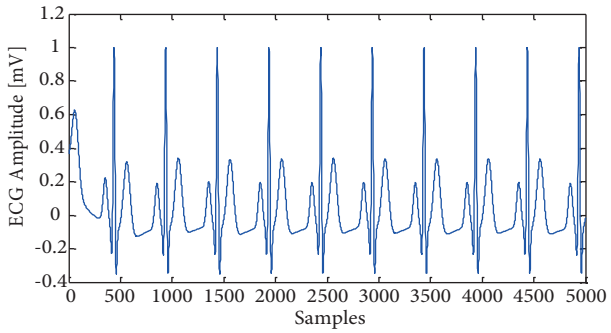

Figure 7. Corrected synthetic ECG signal.

Table 3. Performance evaluation of the proposed method in terms of SNR, MSE, and Imp.

Synthetic ECG with baseline		Corrected synthetic ECG		
Input SNR [dB]	Input MSE	Output SNR [dB]	Output MSE	Imp [dB]
30.89	47.65	38.84	0.00	7.95

from its physiological level reflect an existing acute coronary syndrome, which is one of the most severe forms of heart disease and the main cause of mortality in developed countries [37]. Note that the proposed method did not distort the spectrum of the original ECG signal as we see in Figure 8 and Figure 9; therefore, the method preserves all important clinical information.

4.2. Baseline wander removal from real ECG signal

Figure 10 depicts an example of baseline-corrected real ECG 109.dat [30]. Note that all amplitudes of the real ECG signals used in this investigation are represented in digital format (binary numbers). The recorded ECG signal (105.dat) of the MIT–BIH arrhythmia database [30] was used to assess the performance of the technique under investigation in the case of severe baseline distortion. A highly distorted artificial BW with an amplitude of 100 (digital value) was added. In Figures 11a–11c we show the effectiveness of the method and its success in removing high amplitude baseline distortion from the real ECG signal. It can also be seen that the method extracts both artificial BW and real BW (compare Figures 11a and 11c).

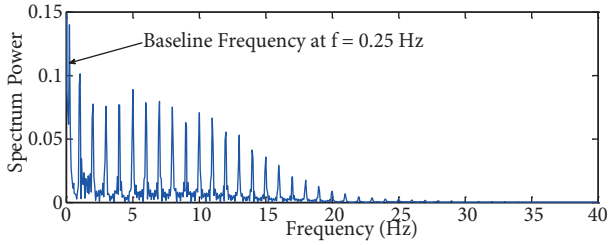

Figure 8. Spectral content of the original ECG signal with the presence of BW at frequency $f_2 = 0.25$ Hz.

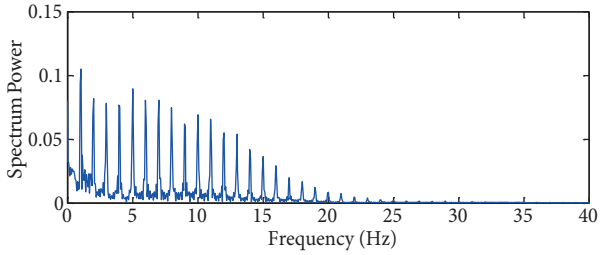

Figure 9. Spectral content of the corrected ECG signal without BW.

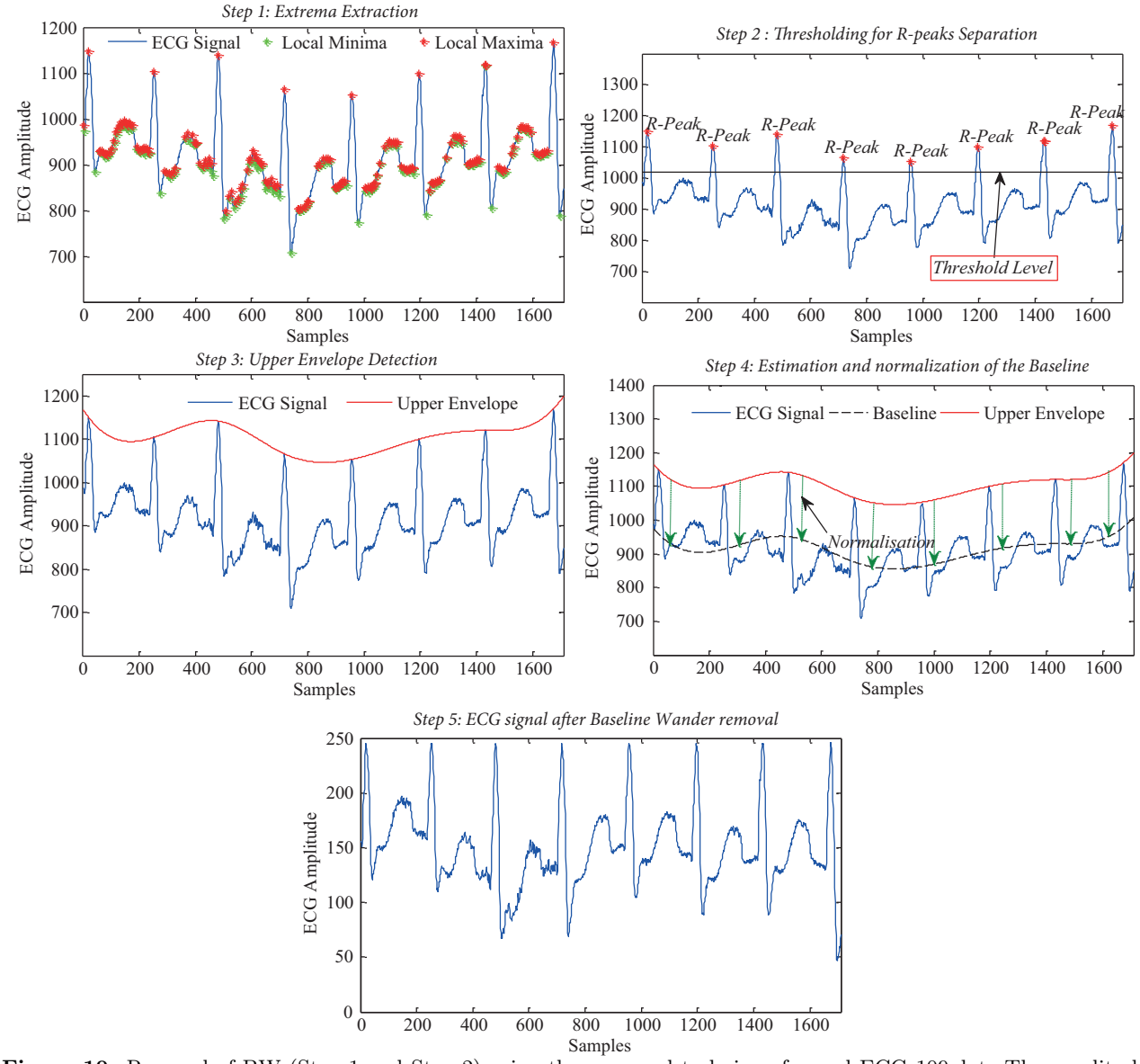

Figure 10. Removal of BW (Step 1 and Step 2) using the proposed technique for real ECG 109.dat. The amplitudes are given in digital format (binary numbers). Removal of BW (Step 3 and Step 4) using the proposed technique for real ECG 109.dat. The amplitudes are given in digital format (binary numbers). Removal of BW (Step 5) using the proposed technique for real ECG 109.dat. The amplitudes are given in digital format (binary numbers).

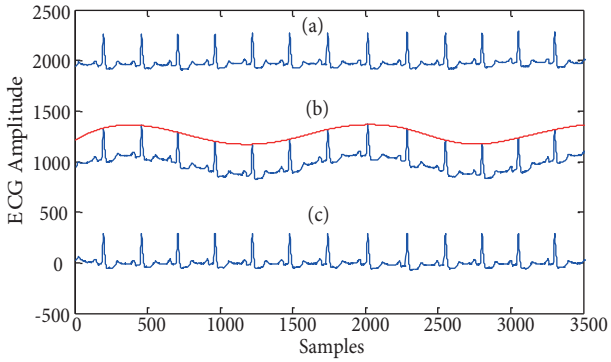

Figure 11. a) 105.dat ECG signal without artificial BW. b) 105.dat ECG signal with artificial BW of amplitude 100. c) Corrected 105.dat ECG signal.

Numerical evaluation of the proposed method is presented in Table 4 in terms of SNR, MSE, and Imp factor criteria, in which significant improvements are noted.

Table 4. Performance evaluation of the proposed method in terms of SNR, MSE, and Imp factor criteria.

Real ECG 105.dat with artificial BW of amplitude 100		Corrected real ECG 105.dat		
Input SNR [dB]	Input MSE	Output SNR [dB]	Output MSE	Imp [dB]
36	15	53.04	0.00	17.04

In what follows, we compare the proposed method against the BW removal methods based on HVD [17] and EMD–MM [8] as described earlier. In order to produce a valid comparison, the method has been simulated with the same parameters, test signals, and noise, and under the same conditions using the same evaluation criteria as those used in the comparison studies with the benchmark methods. The results of the comparison are presented in Table 5. As the findings of the study show, the proposed method provides a better SNR compared to the other methods.

Table 5. Performance evaluation and comparison in terms of SNR criterion.

Recorded ECG signal [30]	Amplitude of the artificial BW	Output SNR [dB]		
		Proposed method	HVD [17]	EMD-MM [8]
100	100	41.82	21.03	20.73
105	100	53.04	30.22	26.27
119	100	55.01	34.20	30.08

To be general, the method will be applied in what follows to many ECG signals selected from the two types of ECG data available from the MIT database [30]: 1) the MIT–BIH Arrhythmia Database and 2) the MIT–BIH Normal Sinus Rhythm Database. As Figures 12–19 demonstrate, the method is very effective for removing the baseline drift.

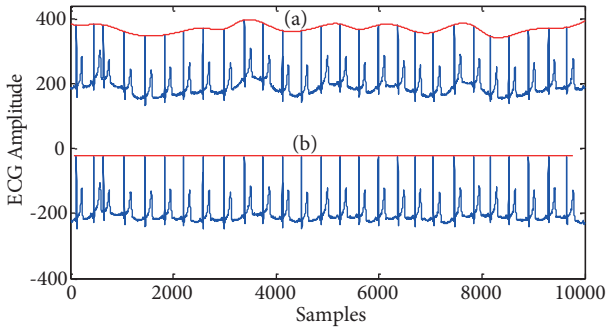

Figure 12. MIT–BIH Arrhythmia Database experiments: a) distorted 113.dat ECG signal, b) corrected 113.dat ECG signal.

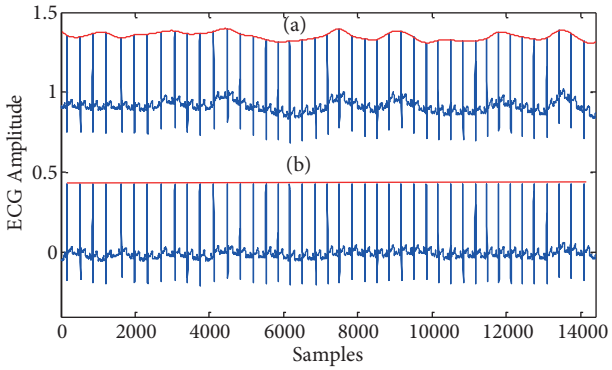

Figure 13. MIT–BIH Arrhythmia Database experiments: a) distorted 115.dat ECG signal, b) corrected 115.dat ECG signal.

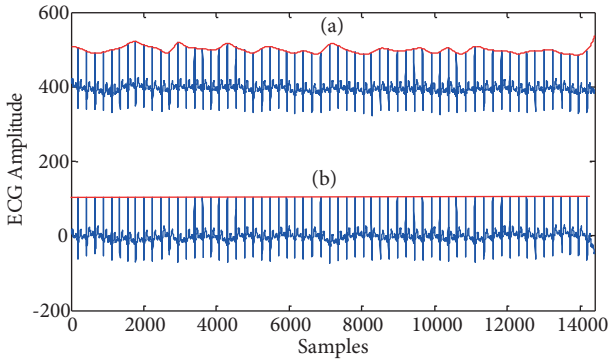

Figure 14. MIT–BIH Arrhythmia Database experiments: a) distorted 209.dat ECG signal, b) corrected 209.dat ECG signal.

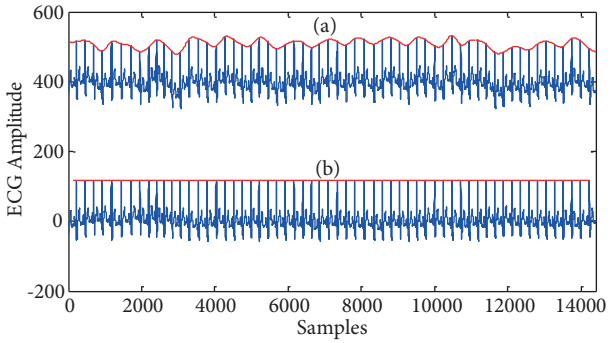

Figure 15. MIT–BIH Arrhythmia Database experiments: a) distorted 212.dat ECG signal, b) corrected 212.dat ECG signal.

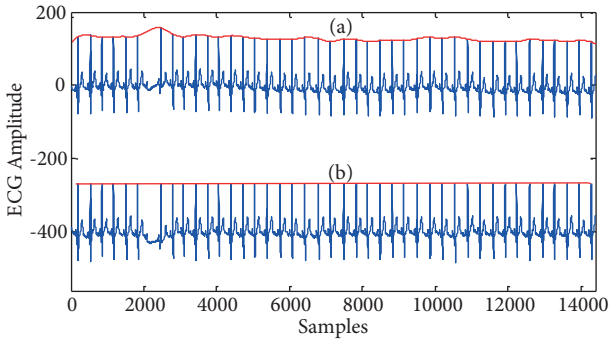

Figure 16. MIT–BIH Arrhythmia Database experiments: a) distorted 231.dat ECG signal, b) corrected 231.dat ECG signal.

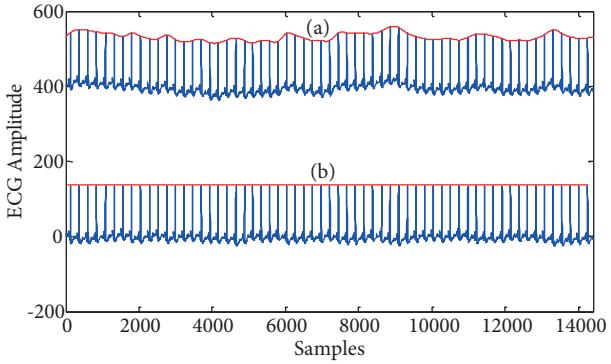

Figure 17. MIT–BIH Arrhythmia Database experiments: a) distorted 234.dat ECG signal, b) corrected 234.dat ECG signal.

5. Conclusion

This study employed an experimental method that used the shape derived from the R-peaks via cubic spline interpolation (upper envelope) to remove the BW from an ECG signal. The results of the simulation indicate that

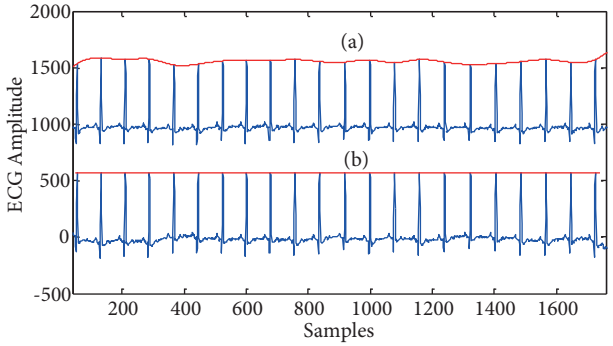

Figure 18. MIT–BIH Normal Sinus Rhythm Database experiments: a) distorted 16265.dat ECG signal, b) corrected 16265.dat ECG signal.

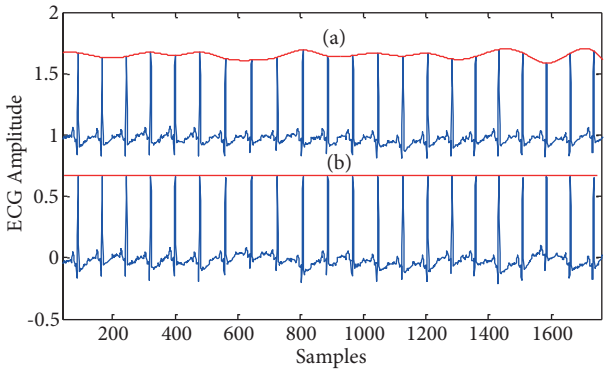

Figure 19. MIT–BIH Normal Sinus Rhythm Database experiments: a) distorted 16273.dat ECG signal, b) corrected 16273.dat ECG signal.

the method used was successful and superior to the established HVD and EMD techniques. The characteristic waveforms of the ECG signal were preserved and the BW was minimized, maintaining the clinically valuable ECG information. Note that the performance of the proposed methods could be further improved by applying better R-peaks detection methods.

References

[1] Fischbach M. Guide Pratique du Cardiaque. Paris, France: Editions Frison-Roche, 2002 (in French).

[2] Venes D. Taber's Cyclopedic Medical Dictionary. New York, NY, USA: FA Davis, 2017.

[3] Saladin KS. Anatomy and Physiology: The Unity of Form and Function. New York, NY, USA: WCB/McGraw-Hill, 1998.

[4] Jenkal W, Latif R, Toumanari A, Dliou A, El B'charri O, Maoulainine FMR. QRS detection based on an advanced multilevel algorithm. Int J Adv Comp App 2016; 1: 253-60.

[5] Hung K, Zhang YT. Implementation of a WAP-based telemedicine system for patient monitoring. IEEE T Inf Technol B 2003; 7: 101-107.

[6] Salvador CH, Carrasco MP, González de Mingo MA, Muñoz Carrero A, Márquez Montes J, Sosa Martín L, Cavero MA, Fernández Lozano I, Monteagudo JL. A GSM and internet services-based system for out of hospital follow-up of cardiac patients. IEEE T Inf Technol B 2005; 9: 73-84.

[7] Rodriguez J, Goni A, Illarramendi A. Real-time classification of ECGs on a PDA. IEEE T Inf TechnoL B 2005; 9: 23-34.

[8] Ji TY, Wu QH. Baseline normalisation of ECG signals using empirical mode decomposition and mathematical morphology. Electron Lett 2008; 44: 82-83.

[9] van Alste JA, van Eck W, Herrmann OE. ECG baseline wander reduction using linear phase filters. Comput Biomed Res 1986; 19: 417-427.

[10] Ciarlini P, Barone P. A recursive algorithm to compute the baseline drift in recorded biological signals. Comput Biomed Res 1988; 21: 221-226.

[11] Meyer CR, Keiser HN. Electrocardiogram baseline noise estimation and removal using cubic splines and state-space computation techniques. Comput Biomed Res 1977; 10: 459-470.

[12] Seygullah HO, Muka HA. A morphology based algorithm for baseline wander elimination in ECG records. In: IEEE 1992 Proceedings of the International Conference Biomedical Engineering Days; 1992; İstanbul, Turkey. pp. 157-160.

[13] Laguna P, Jane R, Caminal P. Adaptive filtering of ECG baseline wander. In: 14th Annual International Conference of the IEEE Engineering in Medicine and Biology Society; 1992. pp. 508-509.

[14] Nitish VT, Zhu YS. Application of adaptive filtering to ECG analysis: noise cancellation and arrhythmia detection. IEEE T Bio-Med Eng 1991; 38: 785-794.

[15] Chen H, Huang K, Jiang Y. Detection of ST segment in electrocardiogram by wavelet transform. Electr Mach Control 2006; 10: 531-533.

[16] Shi L, Yang C, Fei M. Electrocardiogram R-wave and ST segment extraction based on wavelet transform. Chin J Sci Instrum 2008; 29: 804-809.

[17] Sharma H, Sharma KK. Baseline wander removal of ECG signals using Hilbert vibration decomposition. Electron Lett 2015; 51: 447-449.

[18] Fasano A, Villani V. Baseline wander removal for bioelectrical signals by quadratic variation reduction. Signal Process 2014; 99: 48-57.

[19] Sakshi A, Anubha G. Fractal and EMD based removal of baseline wander and powerline interference from ECG signals. Comput Biol Med 2013; 43: 1889-1899.

[20] Zivanovic M, González-Izal M. Simultaneous powerline interference and baseline wander removal from ECG and EMG signals by sinusoidal modeling. Med Eng Phys 2013; 35: 1431-1441.

[21] Leski JM, Henzel N. ECG baseline wander and powerline interference reduction using nonlinear filter bank. Signal Process 2005; 85: 781-793.

[22] Rameshwari M, Cheeran AN, Vaibhav DA. Improved technique to remove ECG baseline wander–application to Pan & Tompkins QRS detection algorithm. Comm Com Inf Sc 2013: 361: 492-499.

[23] Zou C, Qin Y, Sun C, Li W, Chen W. Motion artifact removal based on periodical property for ECG monitoring with wearable systems. Pervasive Mob Comput 2017; 40: 267-278.

[24] Xiao H, Zhong X, Ni Z. Removal of baseline wander from ECG signal based on a statistical weighted moving average filter. J Zhejiang U-Sci C 2011; 12: 397-403.

[25] Blanco-Velasco M, Weng B, Barner KE. ECG signal denoising and baseline wander correction based on the empirical mode decomposition. Comput Biol Med 2008; 38: 1-13.

[26] Gupta P, Sharma KK, Joshi SD. Baseline wander removal of electrocardiogram signals using multivariate empirical mode decomposition. Healthcare Technology Letters 2015; 2: 164-166.

[27] Niederhauser T, Wyss-Balmer T, Haeberlin A, Marisa T, Wildhaber RA, Goette J, Jacomet M, Vogel R. Graphics-processor-unit-based parallelization of optimized baseline wander filtering algorithms for long-term electrocardiography. IEEE T Biomed Eng 2015; 62: 576-1584.

[28] Niederhauser T, Marisa T, Kohler L, Haeberlin A, Wildhaber RA, Abächerli R, Goette J, Jacomet M, Vogel R. A baseline wander tracking system for artifact rejection in long-term electrocardiography. IEEE T Biomed Circ S 2016; 10: 255-265.

[29] Alarka S, Arijit B, Abhijit L. Application of framelet transform in filtering baseline drift from ECG signals. Procedia Technology 2012; 4: 862-866.

[30] Goldberger AL, Amaral LAN, Glass L, Hausdorff JM. {PhysionBank, PhysioToolkit, and PhysioNet}: Components of a new research resource for complex physiologic signals. Circulation 2000; 101: e215-e220.

[31] McSharry PE, Clifford GD, Tarassenko L, Smith L. A dynamical model for generating synthetic electrocardiogram signals. IEEE T Bio-med Eng 2003; 50: 289-294.

[32] Yi L, Liu Z, Wang K, Chen M, Peng S, Zhao W, He J, Zhao G. A new background subtraction method for energy dispersive X-ray fluorescence spectra using a cubic spline interpolation. Nucl Instrum Meth A 2015; 775: 12-14.

[33] Warlar R, Eswaran C. Integer coefficient bandpass filter for the simultaneous removal of baseline wander, 50 and 100 Hz interference from the ECG. Biol Eng Comput 1991; 29: 333-336.

[34] Sörnmo L, Laguna P. ECG Signal Processing. Bioelectrical Signal Processing in Cardiac and Neurological Applications. Amsterdam, the Netherlands: Elsevier Academic Press, 2005.

[35] Azuaje F, Clifford GD, McSharry PE. Advanced Methods and Tools for ECG Data Analysis. Boston, MA, USA: Artech House, Inc., 2006.

[36] Sheffield LT, Berson A, Bragg-Remschel D, Gillette PC, Hermes RE, Hinkle L, Kennedy H, Mirvis DM, Oliver C. Recommendations for standards of instrumentation and practice in the use of ambulatory electrocardiography: AHA Special Report. Circulation 1985; 171: 626A-636A.

[37] Kligfield P, Gettes LS, Bailey JJ, Childers R, Deal BJ, Hancock EW, van Herpen G, Kors JA, Macfarlane P, Mirvis DM et al. Recommendations for the standardization and interpretation of the electrocardiogram: Part I: the electrocardiogram and its technology. Circulation 2007; 115: 1306-1324.